Soft Matter

Accepted Manuscript

ROYAL SOCIETY OF CHEMISTRY

www.rsc.org/softmatter

Journal Name

ARTICLE TYPE

Cite this: DOI: 10.1039/xxxxxxxxxx

Received Date
Accepted Date

DOI: 10.1039/xxxxxxxxxx

www.rsc.org/journalname

Entangled polymer complex as Higgs phenomena†

Ki-Seok Kim,[a] Sandipan Dutta,[b] and YongSeok Jho*[a,b]

We derive an effective Maxwell-London equation for entangled polymer complex under the topological constraint, borrowing the theoretical framework from the topological field theory. We find that the transverse current flux of a test polymer chain, surrounded with the entangled chains, decays exponentially from its centerline position with finite penetration depth, which is analogous to the magnetic-field decay in a superconductor (SC), referred to as Meissner effect. Just as the mass acquirement of photons in SC is the origin of the magnetic-field decay, the polymer earns uncrossable intersections along the chain due to the preserving of linking number, which restricts the deviation of the transverse polymer current in the normal direction. The underlying physics is as follows: Less flexible polymers have stronger current-current correlations, giving rise to heavier effective mass of gauge fields and resulting in shorter decay length. Interestingly, this picture is well incorporated within the most successful phenomenological theory of the, so called, tube model, of which researchers have long pursued its microscopic origin. The correspondence of our equation of motion to the tube model claims that the confining tube potential is a consequence of the topological constraint (linking number). The tube radius is attributed to the decay length. On increasing the effective mass (by strengthen the interaction at uncrossable intersection or number of intersections), the tube becomes narrower. In this argument, the exponential decay of the chain leakage out of the tube is well understood.

1 Introduction

It is an intriguing nature of physics that more than two completely different systems are described within the same mathematical framework. The Chern-Simons theory which was first introduced in string theory by Witten at 1980's[1], turns out to be applicable to the cutting edge problems in condensed matter, such as fractional quantum Hall effect[2] and topological insulator and superconductor[3]. Since Edwards first introduced the topological constraint[4], *i.e.* linking number, to the partition function of the polymer melts, researchers noticed

[a] *Department of Physics, POSTECH, Pohang, Gyeongbuk 790-784, South Korea*
[b] *Asia-Pacific Center for Theoretical Physics, Pohang, Gyeongbuk 790-784, South Korea*
* *E-mail: ysjho@apctp.org*

the potential usefulness to apply the Chern-Simons theory to polymer problems[5,6,7,8]. In those works, the knotted electron's movement is translated to the intersection (entanglement) of polymers. In spite of its mathematical exactness, these approaches were not very successful in polymer entanglement unlike its huge achievement in other fields of physics[9,10]. Main reasons are that the model is still abstract, and the information of microstates is not feasible under the current experimental techniques[9,10].

Surprisingly, long polymer melts, which is one of the most complicated system in polymer physics, is well described by a single body interpretation, *i.e.* tube model[11,12,13]. The tube model is an ansatz to assume that the transverse dynamics of polymer is localized within certain length called tube diameter. It is often expressed as Gaussian distribution from the harmonic confinement potential since Edward suggested it. In addition to many rheological experimental supports[10,14,15,16], recent experiments and simulations verified the validity of the model finding that confinement potential around semi-flexible polymers is combination of linear potential and harmonic one[17,18,19,20]. A recent theory has predicted that the confinement potential is harmonic at very close to the primitive path whereas it is linear at intermediate length scales, which explains recent experiments and simulations well[23,24]. The strength of this intuitive model lies in its universality spanning over the intermediate and long time scale regardless of the detailed chemistry or the structure of the polymer, as long as the polymer is long enough so that we can treat it as a coarse grained random chain with the step size of random work much exceeding the local length scale of the polymer. Since this phenomenological model earned a great success, researchers have been seeking its microscopic origin[20,21,22]. Recent theoretical achievements in this effort have focused on the Langevin approach of statistical mechanics[23,24].

These two approaches, Chern-Simons theory and the tube model, look completely different. However, we believe that the phenomenological theory should be understood from a microscopic theory. The goal of the current work is to pursue this connection.

As Edwards claimed in his pioneering work, polymer conformation can be translated as a classical particle motion[12,25]. In this analogy, time corresponds to the displacement along the chain, and the trajectory of the particle motion is associated with the contour of the polymer. Within this argument, the diffusive motion of a classical particle can be interpreted as a Gaussian distribution of a random polymer chain. To include the entanglement effect, he plugged the topological constraint into the partition function[4]. This entangled polymer system has a similar mathematical structure to the trajectory of a classical particle under a magnetic field following the Biot-Savart law, which allows us to analyze the polymer entanglement in favor of the magnetic-field induction under the constraint of integer linking number. This leads us to construct BF theory[26] that avoids self-linking contrary to Chern-Simons theory[27].

We agree that it is extremely difficult to solve such complicate equations obtained from Chern-Simons theory exactly and provide the correspondence of parameters between the microscopic and phenomenological theories[9,10]. In this respect we adopt a new strategy to make a link between the phenomenological tube model and the microscopic BF theory. Inspired by previous works[5,6,7,8], we derive an effective Maxwell-London equation for the dynamics of entangled polymer melts, starting from the topological BF theory. We interpret the characteristic features of the tube model with this Maxwell-London equation, which leads us to identify the dynamics of entangled polymers with the Higgs phenomena (Meissner effect)[28].

System	Superconductor (SC)	Entangled polymer
Medium	SC vacuum	Entangled polymer complex
	SC boundary	Local centerline position of a chain
Degrees of freedom	Current	Tangential flux of a chain
	External magnetic field	Test chain
	Magnetic field induction	Flux of entangled chains
Topology constraint	Flux quantization	Preserving linking number
Physics	Photon mass	interactions at uncrossable intersections
	Magnetic field penetration	Diffusion of tangential flux
	Decay length	Tube radius

Table 1 An analogy between polymer entanglement (tube model) and superconductor

2 Theoretical Development

2.1 Topological field theory

The polymer density and current for N chains of length L are given by

$$\rho(\mathbf{r}) = \sum_{i=1}^{N} \int_0^L ds \delta(\mathbf{x}_i(s) - \mathbf{r}) \tag{1}$$

$$\mathbf{j}(\mathbf{r}) = \sum_{i=1}^{N} \int_0^L ds \dot{\mathbf{x}}(s) \delta(\mathbf{x}_i(s) - \mathbf{r}). \tag{2}$$

Introducing an artificial electromagnetic vector potential $\mathbf{A}_I(\mathbf{r})$ due to all the polymers except the Ith is given by

$$\nabla \times \mathbf{A}_I(\mathbf{r}) = \sum_{j \neq I} \mathbf{j}_j(\mathbf{r}), \tag{3}$$

where the most general solution to the Eq. (3) is

$$\mathbf{A}_I(\mathbf{r}) = \frac{1}{4\pi} \int \sum_{j \neq I} \mathbf{j}_j(\mathbf{r}') \times \frac{\mathbf{r} - \mathbf{r}'}{|\mathbf{r} - \mathbf{r}'|^3} d\mathbf{r}', \tag{4}$$

it is convenient to express the winding number of the Ith polymer with others as follows

$$N_I = \int d\mathbf{r} \sum_I \mathbf{A}_I(\mathbf{r}) \cdot \mathbf{j}_I(\mathbf{r}). \tag{5}$$

If we consider only two polymer chains for simplicity, it is straightforward to see how Eq. (5) shows the winding number

$$\begin{aligned} N_2 &= \int d\mathbf{r} \mathbf{A}_2(\mathbf{r}) \cdot \mathbf{j}_2(\mathbf{r}) \\ &= \int \frac{1}{4\pi} \int \mathbf{j}_2(\mathbf{r}') \times \frac{\mathbf{r} - \mathbf{r}'}{|\mathbf{r} - \mathbf{r}'|^3} d\mathbf{r}' \cdot \mathbf{j}_1(\mathbf{r}) d\mathbf{r} \\ &= \frac{1}{4\pi} \oint \oint d\mathbf{r}'(s) \times d\mathbf{r}''(s') \cdot \frac{\mathbf{r}'(s) - \mathbf{r}''(s')}{|\mathbf{r}'(s) - \mathbf{r}''(s')|^3}. \end{aligned} \tag{6}$$

Introducing this topological constraint into the partition function for the Ith polymer, we obtain

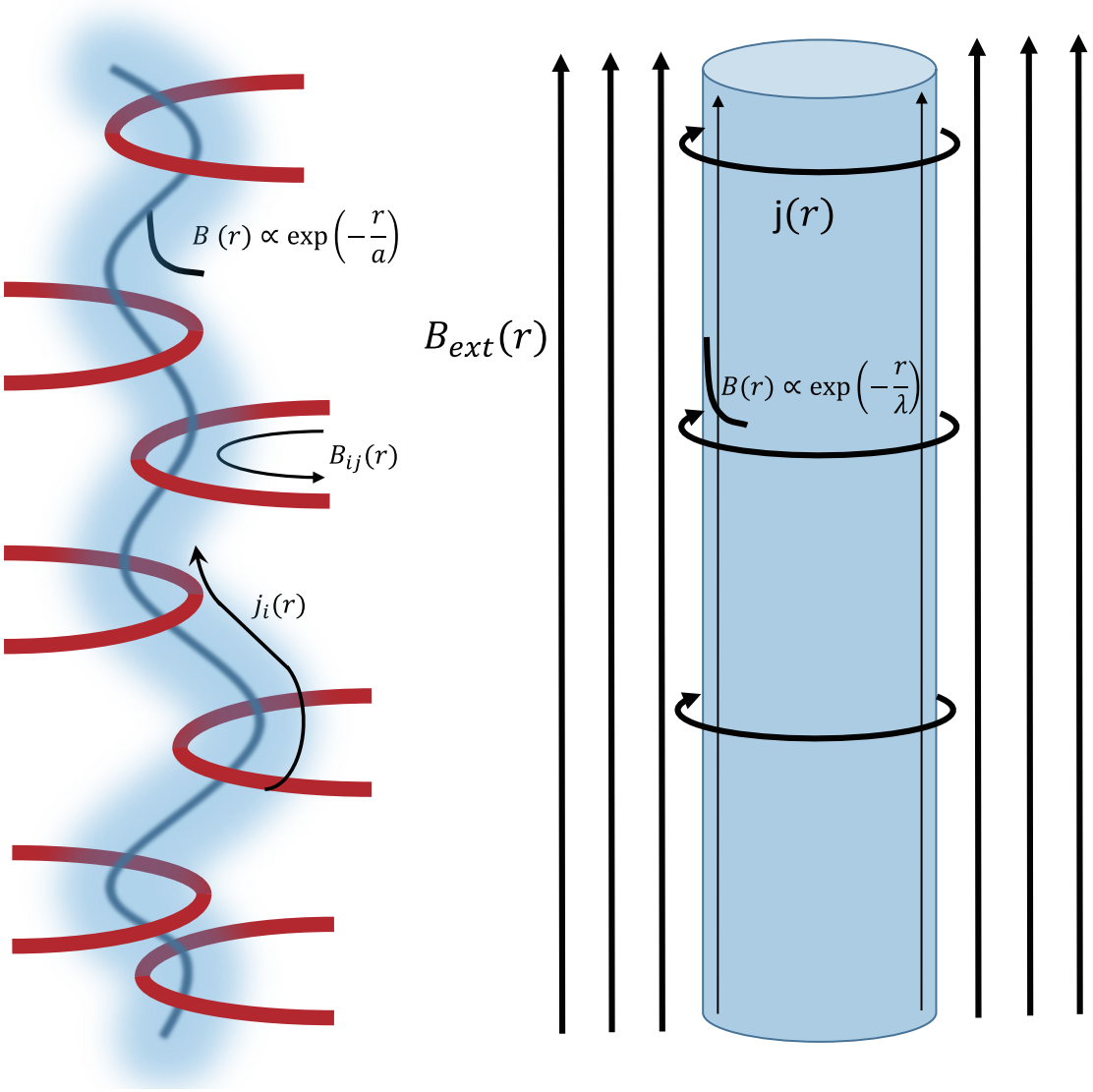

Fig. 1 Schematic illustration of topological constraint of polymer melts. We assume that the number of entanglement is preserved during time scale we are interested in.

$$\mathscr{Z}_I = \sum_{N_I=0}^{\infty} e^{-\mu_I N_I} \sum_{N_{Ij}=0}^{\infty} \delta\Big(\sum_{j\neq I}^{N} N_{Ij} - N_I\Big) \frac{\Pi_{j\neq I}^{N} N_{Ij}!}{N_I!} \left\langle \delta\left(\nabla \times \mathbf{A}_I(\mathbf{r}) - \sum_{j\neq I} \mathbf{j}_j(\mathbf{r})\right) \delta\left(N_I - \int d\mathbf{r} \sum_I \mathbf{A}_I(\mathbf{r}) \cdot \mathbf{j}_I(\mathbf{r})\right) \right\rangle$$

$$= \sum_{N_I=0}^{\infty} e^{-\mu_I N_I} \sum_{N_{Ij}=0}^{\infty} \delta\Big(\sum_{j\neq I}^{N} N_{Ij} - N_I\Big) \frac{\Pi_{j\neq I}^{N} N_{Ij}!}{N_I!} \int \Pi_{i=1}^{N} D\mathbf{X}_i(s) D\mathbf{A}_I(\mathbf{r}) \exp\left\{-\int_0^L ds \sum_{i=1}^{N} \frac{\mathscr{K}}{2} \dot{\mathbf{X}}_i^2(s)\right\}$$

$$\delta\left(\nabla \times \mathbf{A}_I(\mathbf{r}) - \sum_{j\neq I} \mathbf{j}_j(\mathbf{r})\right) \delta\left(N_I - \int d\mathbf{r} \sum_I \mathbf{A}_I(\mathbf{r}) \cdot \mathbf{j}_I(\mathbf{r})\right). \quad (7)$$

N_{Ij} is an integer to represent a Gaussian linking number between the Ith polymer and j_{th} one ($j \neq I$). $N_I = \sum_{j\neq I}^{N} N_{Ij}$ is an integer to express a total Gaussian linking number between the Ith polymer and all others ($j \neq I$). Recall that $\frac{\Pi_{j\neq I}^{N} N_{Ij}!}{N_I!}$ is a standard combinatorial factor counting all possible linking formations between the Ith polymer and all others ($j \neq I$). μ_I is an energy cost per a linking event, which can be determined by microscopic calculations. If this entanglement physics is not taken into account, keeping only one topological sector of $N_I = 0$, we reproduce the conventional expression for the partition function, given by

$$\mathscr{Z}_I = \int \Pi_{i=1}^{N} D\mathbf{X}_i(s) \exp\Big\{ -\int_0^L ds \sum_{i=1}^{N} \frac{\mathscr{K}}{2} \dot{\mathbf{X}}_i^2(s) \Big\}.$$

It is clear that the functional integration of $\int \Pi_{i=1}^{N} D\mathbf{X}_i(s)$ in the presence of $\delta-$function constraints will be much different from that in the absence of them. Although Gaussian polymers have been assumed, this formal expression can be generalized to take into account their interactions.

The $\delta-$function constraints associated with a topological structure is expanded with the relation, $\delta\Big(\mathbf{t}(\mathbf{r})\Big) = \frac{1}{2\pi}\int_{-\infty}^{\infty} dg \exp\Big(-ig\mathbf{t}(\mathbf{r})\Big)$. Then, the partition function is re-expressed as follows

$$\mathscr{Z}_I = \sum_{N_I=0}^{\infty} e^{-\mu_I N_I} \sum_{N_{Ij}=0}^{\infty} \delta\Big(\sum_{j\neq I}^{N} N_{Ij} - N_I\Big) \frac{\Pi_{j\neq I}^{N} N_{Ij}!}{N_I!} \int_{-\infty}^{\infty} dg_I e^{ig_I N_I} \int \Pi_{i=1}^{N} D\mathbf{X}_i(s) D\mathbf{A}_I(\mathbf{r}) D\mathbf{C}_I(\mathbf{r})$$
$$\exp\Big\{ -\Big(\int_0^L ds \sum_{i=1}^{N} \frac{\mathscr{K}}{2} \dot{\mathbf{X}}_i^2(s) - ig_I \int d^d\mathbf{r} \mathbf{j}_I(\mathbf{r}) \cdot \mathbf{A}_I(\mathbf{r}) - i \int d^d\mathbf{r} \mathbf{C}_I(\mathbf{r}) \cdot \sum_{j\neq I}^{N} \mathbf{j}_j(\mathbf{r}) + i \int d^d\mathbf{r} \mathbf{C}_I(\mathbf{r}) \cdot [\nabla \times \mathbf{A}_I(\mathbf{r})] \Big) \Big\}, \quad (8)$$

where $\mathscr{K}$ is a spring constant of harmonic potential in connectivity, g_I is a Lagrange multiplier field to impose the constraint $\delta\left(N_I - \int d\mathbf{r}\sum_I \mathbf{A}_I(\mathbf{r})\cdot\mathbf{j}_I(\mathbf{r})\right)$ and $\mathbf{C}_I(\mathbf{r})$ is an auxiliary gauge field to impose the constraint $\delta\left(\nabla\times\mathbf{A}_I(\mathbf{r}) - \sum_{j\neq I}\mathbf{j}_j(\mathbf{r})\right)$. In other words, the functional integration for $\mathbf{C}_I(\mathbf{r})$ recovers the constraint of $\delta\left(\nabla\times\mathbf{A}_I(\mathbf{r}) - \sum_{j\neq I}\mathbf{j}_j(\mathbf{r})\right)$ and the integration of g_I keeps $\delta\left(N_I - \int d\mathbf{r}\sum_I \mathbf{A}_I(\mathbf{r})\cdot\mathbf{j}_I(\mathbf{r})\right)$. It is useful to re-express the constraints as current induction form, $\frac{g_I}{2}\mathbf{j}_I(\mathbf{r}) = \nabla\times\mathbf{C}_I(\mathbf{r})$ and $\sum_{j\neq I}\mathbf{j}_j(\mathbf{r}) = \nabla\times\mathbf{A}_I(\mathbf{r})$. It is interesting to notice that the effect of topological constraints from the entangled polymers w.r.t. I_{th} polymer is coarse grained into $\mathbf{j}_I(\mathbf{r})$. This process resembles the idea of tube model which coarse grains the interaction from the entangled polymers as an effective potential well of confining tube w.r.t. the test chain.

It is straightforward to write down the canonical partition function for N polymers, given by

$$\begin{aligned}\mathscr{Z}_N &= \sum_{N_G=0}^{\infty} e^{-\mu_G N_G}\sum_{N_I=0}^{\infty}\delta\Big(N_G - \sum_{I=1}^{N}N_I\Big)\frac{\Pi_{I=1}^{N}N_I!}{N_G!}\sum_{N_{Ij}=0}^{\infty}\delta\Big(N_I - \sum_{j\neq I}^{N}N_{Ij}\Big)\frac{\Pi_{j\neq I}^{N}N_{Ij}!}{N_I!}\int_{-\infty}^{\infty}\Pi_{I=1}^{N}dg_I e^{i\Sigma_{I=1}^{N}g_I N_I}\\ &\int\Pi_{I=1}^{N}D\mathbf{X}_I(s)D\mathbf{A}_I(\mathbf{r})D\mathbf{C}_I(\mathbf{r})\exp\Big\{-\sum_{I=1}^{N}\Big(\int_0^L ds\frac{\mathscr{K}}{2}\dot{\mathbf{X}}_I^2(s) - \frac{i}{2}\int d^d\mathbf{r}g_I\mathbf{j}_I(\mathbf{r})\cdot\mathbf{A}_I(\mathbf{r}) - i\int d^d\mathbf{r}\mathbf{C}_I(\mathbf{r})\cdot\sum_{j\neq I}^{N}\mathbf{j}_j(\mathbf{r})\\ &+i\int d^d\mathbf{r}\mathbf{C}_I(\mathbf{r})\cdot[\nabla\times\mathbf{A}_I(\mathbf{r})]\Big)\Big\},\end{aligned} \tag{9}$$

where $N_G = \sum_{I=1}^{N}N_I$ is the total Gaussian linking number and μ_G is an energy cost per a linking event. Since we should count others as the Ith polymer, the combinatorial factor of $\frac{\Pi_{I=1}^{N}N_I!}{N_G!}$ appears. The partition function may be more manageable in a form of the grand canonical partition function, given by

$$Z_{GC} = \sum_{N=0}^{\infty}\frac{e^{-\mu N}}{N!}Z_N, \tag{10}$$

where μ is a chemical potential for a polymer.

An essential feature in this formulation lies in the so called BF term, given by

$$\mathscr{S}_{BF} = i\int d^d\mathbf{r}\sum_{I=1}^{N}\mathbf{C}_I(\mathbf{r})\cdot[\nabla\times\mathbf{A}_I(\mathbf{r})], \tag{11}$$

which describes mutual entanglement of polymers. In addition to the BF term, the dynamics of the fluctuating polymers will give rise to the Maxwell dynamics for the emergent gauge fields of $\mathbf{A}_I(\mathbf{r})$ and $\mathbf{C}_I(\mathbf{r})$. In other words, the functional integration of $\int\Pi_{I=1}^{N}D\mathbf{X}_I(s)$ results in kinetic-energy terms for $\mathbf{A}_I(\mathbf{r})$ and $\mathbf{C}_I(\mathbf{r})$. This may be regarded as the effect of renormalization for the dynamics of photons from the dynamics of electrons in the theory of quantum electrodynamics[29], where the functional integration for electron fields causes renormalization in the kinetic energy of photon fields, referred to as random phase approximation.

More explicitly, we consider

$$Z_{GC} = \sum_{N=0}^{\infty} \frac{e^{-\mu N}}{N!} \sum_{N_G=0}^{\infty} e^{-\mu_G N_G} \sum_{N_I=0}^{\infty} \delta\Big(N_G - \sum_{I=1}^{N} N_I\Big) \frac{\Pi_{I=1}^{N} N_I!}{N_G!} \sum_{N_{Ij}=0}^{\infty} \delta\Big(N_I - \sum_{j\neq I}^{N} N_{Ij}\Big) \frac{\Pi_{j\neq I}^{N} N_{Ij}!}{N_I!}$$

$$\int_{-\infty}^{\infty} \Pi_{I=1}^{N} dg_I e^{i\Sigma_{I=1}^{N} g_I N_I} \int \Pi_{I=1}^{N} D\mathbf{A}_I(\mathbf{r}) D\mathbf{C}_I(\mathbf{r}) \exp\Big\{-i \sum_{I=1}^{N} \int d^d\mathbf{r} \mathbf{C}_I(\mathbf{r}) \cdot [\nabla \times \mathbf{A}_I(\mathbf{r})]\Big\}$$

$$\Big\langle \exp\Big\{ i \sum_{I=1}^{N} \Big(\frac{1}{2} \int d^d\mathbf{r} g_I \mathbf{j}_I(\mathbf{r}) \cdot \mathbf{A}_I(\mathbf{r}) + \int d^d\mathbf{r} \mathbf{C}_I(\mathbf{r}) \cdot \sum_{j\neq I}^{N} \mathbf{j}_j(\mathbf{r}) \Big) \Big\} \Big\rangle, \tag{12}$$

where $\langle e^{-S_{int}} \rangle = \int \Pi_{I=1}^{N} D\mathbf{X}_I(s) \exp\Big\{ -\sum_{I=1}^{N} \int_0^L ds \frac{\mathscr{K}}{2} \dot{\mathbf{X}}_I^2(s) \Big\} e^{-S_{int}}$.

Resorting to the cumulant expansion of $\langle e^{-S_{int}} \rangle \approx e^{-\langle S_{int}\rangle + \frac{1}{2}(\langle S_{int}^2\rangle - \langle S_{int}\rangle^2)}$, we obtain

$$Z_{GC} = \sum_{N=0}^{\infty} \frac{e^{-\mu N}}{N!} \sum_{N_G=0}^{\infty} e^{-\mu_G N_G} \sum_{N_I=0}^{\infty} \delta\Big(N_G - \sum_{I=1}^{N} N_I\Big) \frac{\Pi_{I=1}^{N} N_I!}{N_G!} \sum_{N_{Ij}=0}^{\infty} \delta\Big(N_I - \sum_{j\neq I}^{N} N_{Ij}\Big) \frac{\Pi_{j\neq I}^{N} N_{Ij}!}{N_I!}$$

$$\int_{-\infty}^{\infty} \Pi_{I=1}^{N} dg_I e^{i\Sigma_{I=1}^{N} g_I N_I} \int \Pi_{I=1}^{N} D\mathbf{A}_I(\mathbf{r}) D\mathbf{C}_I(\mathbf{r}) \exp\Big\{-i \sum_{I=1}^{N} \int d^d\mathbf{r} \mathbf{C}_I(\mathbf{r}) \cdot [\nabla \times \mathbf{A}_I(\mathbf{r})]\Big\}$$

$$\exp\Big\{ -\frac{1}{2} \Big(\sum_{I=1}^{N} \sum_{I'=1}^{N} \frac{1}{4} \int d^d\mathbf{r} \int d^d\mathbf{r}' g_I g_{I'} \mathbf{A}_I^k(\mathbf{r}) \Big\langle \mathbf{j}_I^k(\mathbf{r}) \mathbf{j}_{I'}^{k'}(\mathbf{r}') \Big\rangle_c \mathbf{A}_{I'}^{k'}(\mathbf{r}') + \int d^d\mathbf{r} \int d^d\mathbf{r}' \mathbf{C}_I^k(\mathbf{r}) \Big\langle \sum_{j\neq I}^{N} \sum_{j'\neq I'}^{N} \mathbf{j}_j^k(\mathbf{r}) \mathbf{j}_{j'}^{k'}(\mathbf{r}') \Big\rangle_c \mathbf{C}_{I'}^{k'}(\mathbf{r}') \Big) \Big\}, \tag{13}$$

where $\langle \mathscr{O}^2 \rangle_c = \langle \mathscr{O}^2 \rangle - \langle \mathscr{O} \rangle^2$. The superscript k in vector potentials and currents represents their vector components of x, y, z. The cross-coupling term between $\mathbf{A}_I^k(\mathbf{r})$ and $\mathbf{C}_I^{k'}(\mathbf{r}')$ does not arise because of $\Big\langle \mathbf{j}_I^k(\mathbf{r}) \sum_{j\neq I}^{N} \mathbf{j}_j^{k'}(\mathbf{r}') \Big\rangle_c = 0$.

Now, our real problem is to evaluate the current-current correlation functions. All physical properties of polymer dynamics are introduced into these correlations. For example, the flexibility of the polymer and their interactions will modify their current-current correlations. In the present study we do not perform this serious procedure explicitly. Instead, we take into account only the Maxwell-type dynamics as the zeroth-order approximation. We emphasize that this Maxwell dynamics of gauge fields resulting from dynamics of polymers can be easily modified via interactions between polymer segments. As a result, we obtain the so called BF-Maxwell theory as an effective description for the dynamics of entangled polymers, given by

$$\mathscr{S}_{eff} = \int d^d\mathbf{r} \sum_{I=1}^{N} \Big(\frac{1}{2e_c^2}[\mathbf{E}^2_{\mathbf{C}_I}(\mathbf{r}) - \mathbf{B}^2_{\mathbf{C}_I}(\mathbf{r})] + \frac{1}{2e_a^2}[\mathbf{E}^2_{\mathbf{A}_I}(\mathbf{r}) - \mathbf{B}^2_{\mathbf{A}_I}(\mathbf{r})] + i\mathbf{C}_I(\mathbf{r}) \cdot [\nabla \times \mathbf{A}_I(\mathbf{r})] \Big), \tag{14}$$

where both effective coupling constants of e_c^2 and e_a^2 are proportional to g_I^2 since these contributions originate from the fluctuating polymers. We recall that they are determined by the current-current correlation[30]. Considering

$$\begin{aligned} \partial_t \quad &\longrightarrow \quad \int_0^L ds \frac{d}{ds} = \int_0^L ds \sum_{i=1}^{N} \frac{d\mathbf{X}_i(s)}{ds} \cdot \frac{\partial}{\partial \mathbf{X}_i(s)} \\ &= \quad \int_0^L ds \sum_{i=1}^{N} \int d^d\mathbf{r} \delta^{(3)}(\mathbf{r} - \mathbf{X}_i(s)) \dot{\mathbf{X}}_i(s) \cdot \nabla_{\mathbf{r}}, \end{aligned}$$

we obtain

$$\partial_t \longrightarrow \sum_{i=1}^{N} \mathbf{j}_i(\mathbf{r}) \cdot \nabla_{\mathbf{r}}.$$

Then, effective electric and magnetic fields are given by

$$\begin{aligned} \mathbf{E}_{\mathbf{C}_I}(\mathbf{r}) &= -\partial_t \mathbf{C}_I(\mathbf{r}) \equiv -\sum_{i=1}^{N} \mathbf{j}_i(\mathbf{r}) \cdot \nabla \mathbf{C}_I(\mathbf{r}), \\ \mathbf{B}_{\mathbf{C}_I}(\mathbf{r}) &= \nabla \times \mathbf{C}_I(\mathbf{r}) \end{aligned} \tag{15}$$

for $\mathbf{C}_I(\mathbf{r})$ and

$$\begin{aligned} \mathbf{E}_{\mathbf{A}_I}(\mathbf{r}) &\equiv -\partial_t \mathbf{A}_I(\mathbf{r}) = -\sum_{i=1}^{N} \mathbf{j}_i(\mathbf{r}) \cdot \nabla \mathbf{A}_I(\mathbf{r}), \\ \mathbf{B}_{\mathbf{A}_I}(\mathbf{r}) &= \nabla \times \mathbf{A}_I(\mathbf{r}), \end{aligned} \tag{16}$$

for $\mathbf{A}_I(\mathbf{r})$.

2.2 Maxwell-London equation

Substituting Eqs. (15) and (16) into Eq. (14) and applying the least action principle to the BF-Maxwell action for gauge fields, it is straightforward to derive the following equation of motion

$$\begin{aligned} -\frac{1}{e_c^2}\sum_{i=1}^{N}\sum_{i'=1}^{N}[\mathbf{j}_i(\mathbf{r})\cdot\nabla][\mathbf{j}_{i'}(\mathbf{r})\cdot\nabla]\mathbf{C}_I(\mathbf{r}) + \frac{1}{e_c^2}\nabla^2\mathbf{C}_I(\mathbf{r}) - \frac{1}{e_c^2}\nabla\nabla\cdot\mathbf{C}_I(\mathbf{r}) &= -i\nabla\times\mathbf{A}_I(\mathbf{r}), \\ -\frac{1}{e_a^2}\sum_{i=1}^{N}\sum_{i'=1}^{N}[\mathbf{j}_i(\mathbf{r})\cdot\nabla][\mathbf{j}_{i'}(\mathbf{r})\cdot\nabla]\mathbf{A}_I(\mathbf{r}) + \frac{1}{e_a^2}\nabla^2\mathbf{A}_I(\mathbf{r}) - \frac{1}{e_a^2}\nabla\nabla\cdot\mathbf{A}_I(\mathbf{r}) &= -i\nabla\times\mathbf{C}_I(\mathbf{r}). \end{aligned} \tag{17}$$

If we focus on the linear regime for the gauge dynamics, we are allowed to ignore the first term. Because the polymer current can be expressed in terms of gauge potentials, referred to as constituent equations, the first term gives rise to higher-order dynamics of gauge fields, and is ignored. Our final result guarantees the self-consistency of this assumption. Since gauge fields turn out to be massive

due to the topological BF term, higher order terms in gauge fluctuations are suppressed. This may be regarded to be nothing but the Ohm's law in metals although it is not clear how to construct precise constituent equations at the present situation, where the dynamic information of the entangled polymers should be incorporated. As a result, we obtain

$$\frac{1}{e_c^2}\nabla^2\mathbf{C}_I(\mathbf{r}) - \frac{1}{e_c^2}\nabla\nabla\cdot\mathbf{C}_I(\mathbf{r}) = -i\nabla\times\mathbf{A}_I(\mathbf{r}),$$
$$\frac{1}{e_a^2}\nabla^2\mathbf{A}_I(\mathbf{r}) - \frac{1}{e_a^2}\nabla\nabla\cdot\mathbf{A}_I(\mathbf{r}) = -i\nabla\times\mathbf{C}_I(\mathbf{r}) \quad (18)$$

Taking the Coulomb gauge of $\nabla\cdot\mathbf{C}_I(\mathbf{r}) = 0$ and $\nabla\cdot\mathbf{A}_I(\mathbf{r}) = 0$ and applying $\nabla\times$ to both sides of equations, we find the Maxwell-London equation

$$\frac{1}{e_c^2}\nabla^2\mathbf{B}_{\mathbf{C}_I}(\mathbf{r}) = e_a^2\mathbf{B}_{\mathbf{C}_I}(\mathbf{r}),$$
$$\frac{1}{e_a^2}\nabla^2\mathbf{B}_{\mathbf{A}_I}(\mathbf{r}) = e_c^2\mathbf{B}_{\mathbf{A}_I}(\mathbf{r}). \quad (19)$$

Recall

$$\mathbf{B}_{\mathbf{A}_I}(\mathbf{r}) = \sum_{j\neq I}^{N}\mathbf{j}_j(\mathbf{r}), \qquad \mathbf{B}_{\mathbf{C}_I}(\mathbf{r}) = \frac{g_I}{2}\mathbf{j}_I(\mathbf{r}). \quad (20)$$

We write down the Maxwell-London equation in a more suggestive fashion

$$\left(D\nabla^2 - M^2(\mathbf{r})\right)\mathbf{B}(\mathbf{r}) = 0, \quad (21)$$

where the diffusion coefficient of D is introduced for physical interpretation. We emphasize that the flexibility of the polymer and their interactions are encoded in the mass term ($M(\mathbf{r})$) through the current-current correlation. For example, the rigidity of the polymer causes heavier effective mass of gauge fields, and thus the diffusive motion is more strongly suppressed for semi-flexible polymers than flexible ones. It is interesting to notice that $M(\mathbf{r})$ can be identified with an effective mass of photons inside SC that corresponds to an inverse of the penetration depth of magnetic fields. In the setup of the BF theory it is proportional to g_I^2, where g_I is the coupling function to enforce the constraint of the Gaussian linking number. Within our semiclassical framework, it can be determined by the saddle-point approximation for the resulting free energy. This procedure may be one of the most complex parts in our analysis. In the present study we do not perform this saddle point analysis and take the mass parameter as a function of the distance away from the centerline position of a test polymer. In the language of polymers, the penetration depth is read as a decay length of the transverse distribution of the test polymer current from its local centerline position. The mass may be understood as interactions at the uncrossable intersections along the contour. In SC, the dissipationless current is induced to cancel the magnetic field inside as seen in Fig. 1, leaving the shallow penetration depth at the surface. In polymer melts, entangled chains (with a test chain) restrict large deviations of the test chain to the normal direction. Thus, we conclude that the decay of the transverse polymer current in the normal direction is an essential character resulting from the topological constraint. This picture is well incorporated in the tube model. In comparison with the tube model, the backbone of the tube is a centerline position, and the radius of the tube corresponds to the decay length (the penetration depth in SC). In this argument, the exponential decay of the chain leakage out of the tube is well understood.

3 Comparison with numerical results

3.1 Method

The transverse current flux distribution is obtained by using computer simulation and compared with the theoretical results that predict a linear combination of exponential decaying and the Gaussian distribution. The centerline of the tube is approximated as a primitive path from energy minimiza-

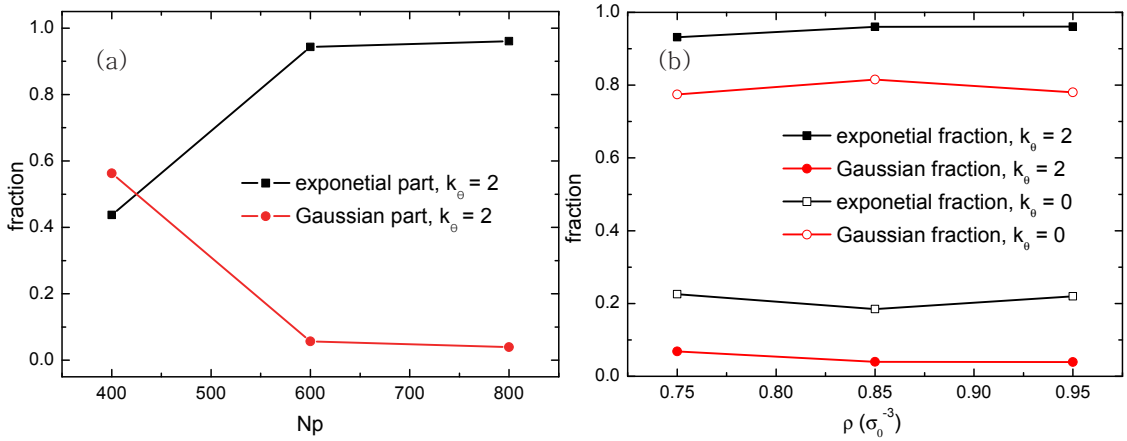

Fig. 3 The areal fractions of Gaussian distribution and the exponential decaying function are plotted as functions of (a) N_p (b) k_θ, and ρ when the transverse distributions are fitted with linear combination of Gaussian distribution and exponential decaying function.

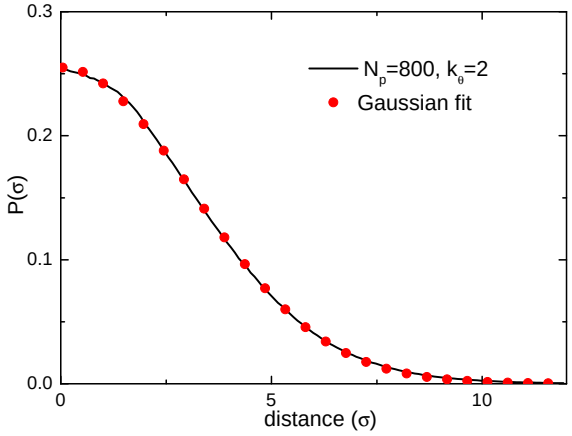

Fig. 2 The transverse distribution of the chain is plotted at very low polymer density of 0.01. The distribution is fitted with Gaussian perfectly except the center of local centerline position where the attraction of Lennard-Jones interaction affects.

tion[22]. The effective potential and the chain flux distribution is measured by using direct tube sampling (DTS)[20].

In order to obtain the melt conformation we adopt slow push-off procedure of Auhl's[31]. Then molecular dynamics simulation is carried out based on the coarse-graining entanglement model developed by Kremer and Grest[32]. Temperature of the system is kept to be $297K$ using the Langevin equation.

Three interactions are considered to reflect the monomer size, chain connectivity, and the bending rigidity of the polymer. The interaction between monomers is incorporated in a Lennard-Jones (LJ) potential,

$$U_{LJ} = \begin{cases} 4\varepsilon\left\{\left(\frac{\sigma_0}{r}\right)^{12} - \left(\frac{\sigma_0}{r}\right)^{6} + \frac{1}{4}\right\} & r < r_c \\ 0 & r \geq r_c \end{cases} \quad (22)$$

where, $r_c = 2^{\frac{1}{6}}\sigma_0$. σ_0 is a length unit in LJ model representing a diameter of monomer.

The chain is sustained by a FENE potential,

$$U_{FENE} = \begin{cases} -0.5kR_0^2 \ln\left(1-(r/R_0)^2\right) & r < R_0, \\ \infty & r \geq R_0 \end{cases} \quad (23)$$

where $R_0 = 1.5\sigma_0$. ε is an energy unit in LJ potential. To adjust the stiffness of the chain, we add a

bending potential,

$$U_{bend} = k_\theta (1 - \cos\theta) \quad (24)$$

where, k_θ is the bending stiffness, and the angle θ is defined as $\cos\theta_i = \frac{(\vec{\mathbf{r}}_i - \vec{\mathbf{r}}_{i-1})\cdot(\vec{\mathbf{r}}_{i+1} - \vec{\mathbf{r}}_i)}{|(\vec{\mathbf{r}}_i - \vec{\mathbf{r}}_{i-1})||(\vec{\mathbf{r}}_{i+1} - \vec{\mathbf{r}}_i)|}$. When $k_\theta = 0$, the chain is flexible. Chain becomes stiff as increasing the bending rigidity, for example at $k_\theta = 2$, the characterisitic ratio C_∞ is about 3.4 considered as semiflexible polymer. According to the reference[32] N_e^P is 65 for $k_\theta = 0$, and 23 for $k_\theta = 2$. As Kremer and Grest pointed out at $\varepsilon = k_B T$, and $k = 30\frac{\varepsilon}{\sigma_0^2}$ there is a huge energy barrier ($\simeq 70 k_B T$) for two chains to cross. This ensures the uncrossability of the chain.

A computational time of the regular MD or MC simulations for entangled long polymer melts takes very long[31]. Considering the relaxation time, which scales as about N_p^3 (N_p is polymerization degree.) and at least N_p^4 in computational cost[31], we only are able to simulate short chain of polymer ($N_p \leq 800$). The length and time are normalized by σ_0, and $\tau_0 = \sigma_0(m/\varepsilon)^{1/2}$, respectively ($m$ is a mass of monomer.). The friction coefficient for Gaussian noise is set $0.5m/\tau_0$. The time step is chosen as $dt = 0.01\tau_0$. To properly equilibrate the system, we adjust the simulation time scale to exceed the longest relaxation time (the disengagement time, $\tau_d = 4.5(N_p^3/N_e)\tau_0$). 10^8 time steps are used for equilibration, and another 10^8 time steps are used for the data production.

The transverse distribution of the chain from its centerline is measured within the constraint release time. For this purpose, we apply the direct tube sampling (DTS)[20]. We follow Zhou and Larson's process[2]. In order to keep the topological constraint preventing the reptation motion, disengagement or constraint release, we quench the ends of the polymers. In this way, we only consider the high-frequency Rouse motion and the transverse diffusion. In DTS, we find the primitive paths of each conformation that are saved during production stage. At every $1000\tau_0$ we collect the configurations for 200 times, *i.e.* for $2\times10^5\tau_0$ steps.

The centerline is approximated as primitive path from energy minimization. By cooling the temperature of the system to $T \simeq 0$, we find out the energy minimized conformation of the polymer[33]. Then, we return back to the normal temperature and measure the deviation of the chain from the primitive path. The distance of the monomer from primitive path is calculated by measuring the distance between monomer and its projection onto the surface[20]. The location of projection between two adjacent monomers should not be separated by 15 monomer distance.

3.2 Numerical Results

Linking number is preserved only for an intermediate time scale $\tau_d \gg t \gg \tau_R(\simeq 1.5N_p^2\tau_0)$ when the topological constraint affects the transverse chain dynamics but the longitudinal reptation motion, disengagement or constraint release are still suppressed. Incorporating the dynamical aspects of the entangled polymers into the static Maxwell-London equation for this regime, we propose an extended Maxwell-London equation

$$\partial_t \mathbf{B}(\mathbf{r},t) = D\nabla^2\mathbf{B}(\mathbf{r},t) - M^2(\mathbf{r})\mathbf{B}(\mathbf{r},t), \quad (25)$$

where

$$\mathbf{B}(\mathbf{r},t) \propto \mathbf{j}(\mathbf{r},t) = \int_0^L ds \frac{d}{ds}\mathbf{X}(s,t)\delta^{(3)}(\mathbf{X}(s,t) - \mathbf{r}). \quad (26)$$

Within this time scale, the distribution of the intersections is not fully uniform over the chain, but localized. For the part of the chain far from the intersection, the diffusive motion would be dominant, *i.e.* the polymer current of $\mathbf{J_I}$ will follow the Gaussian distribution, described by $\partial_t\mathbf{B}(\mathbf{r},t) = D\nabla^2\mathbf{B}(\mathbf{r},t)$ especially, near $|\mathbf{r}| \approx 0$. In Fig.2, this idea is verified

from the numerical simulation. At very low polymer density ($\rho = 0.01$), the transverse distribution fits very well with a Gaussian distribution which is a consequence of the diffusive motion. The diffusion time scale (or relaxation time under quenched ends) is dependent on the chain length between intersections $\left(r_D \simeq \sqrt{N_e}\sigma_0\right)$ which is nothing but width of the Gaussian distribution. On the other hand, near the intersections the fluctuations of the test polymer will be suppressed. As a result, we expect a static solution in which the mass term is dominant, described by the Maxwell-London equation. The decay length λ_d is about $\frac{\sqrt{D}}{M(\mathbf{r})}$. It is important to notice that $M(\mathbf{r})$ is determined by the current-current correlation. The stronger current-current correlation in semi-flexible polymers results in heavier effective mass ($M(\mathbf{r})$) compared to flexible ones, *i.e.* shorter decay length for less flexible polymers. In a nutshell, the tube diameter can be justified as a dominant decaying length scale between r_D and λ_d or their combination. In our derivation, the mass term (current-current correlation) is dependent on the energy of linking events, and its spatial frequency (inverse entanglement length), *i.e.* the mass term is dominant when the interaction energy at intersection is strong and linking number per chain length is large.

Unlike Gaussian distribution in dilute polymer solution (Fig.2), the distribution cannot be fit with pure Gaussian distribution anymore in high polymer concentration. Instead they are fit with a linear combination of the Gaussian distribution and the exponential decaying function as predicted in the theory. The areas of the Gaussian part and the exponential decaying part are plotted in Fig. 3 by varying the chain length, stiffness and concentration which change effective mass term through the linking number and the interaction energy at intersection. This will contrast the contribution of entanglement with respect to the diffusive motion. In Fig. 3-(a) we plot the transverse distribution of the chain as a function of the normal distance σ from its centerline varying N_p (at $\rho = 0.85\sigma_0^{-3}$). Although the ρ is the same, longer chain has more intersections per chain (larger linking number), which induces tighter networks. The interaction energy at the intersections is expected to be stronger than shorter chain (corresponding to heavier effective mass). As a result, the Gaussian part is more important for short chain but exponential part is dominant for long chain ($N_p \geq 600$) as seen in Fig. 3-(a).

In Fig. 3-(b), we compare the Gaussian contribution with the exponential contribution as functions of the concentration ρ and the bending rigidity k_θ. On increasing k_θ, a chain transits from a flexible chain to a semi-flexible chain, which enhances the current-current correlations. As a result, the effective mass term increases in extended Maxwell-London equation. Indeed faster decay of the transverse distribution, which is proportional to the inverse effective mass, is observed for $k_\theta = 2$ regardless ρ than $k_\theta = 0$. At $k_\theta = 0$ (flexible polymer with larger N_e), the Gaussian part is still dominant, although there exists the exponential decaying fraction.

3.3 Towards the second "quantization"

Our phenomenological Maxwell-London equation based on the topological BF theory seems to be not inconsistent with the tube model. However, there still exist important unanswered questions, which may be difficult to solve within the present formulation. For example, it is not clear how to express the mass parameter as a function of measurable physical quantities. We point out that this fundamental difficulty of our formulation results from the fact that the theory is written in the language of the first "quantization". We need to represent the BF theory in the second-quantization formulation, where not only gauge dynamics but also polymer dynamics is expressed in terms of field variables instead of the position variable. This work has been performed before[34], where the generating function of

$$W = \int Dq(\mathbf{r},s)\exp\Big\{-\int_0^N ds\int d^3\mathbf{r}\frac{1}{2}q(\mathbf{r},s)(\partial_s - D\nabla_{\mathbf{r}}^2)q(\mathbf{r},s)\Big\} \tag{27}$$

leads to the Edwards-Anderson equation

$$\partial_s q(\mathbf{r},s) = D\nabla_{\mathbf{r}}^2 q(\mathbf{r},s) \tag{28}$$

in the saddle-point analysis and an internal energy

$$E = -\lim_{N\to\infty}\frac{1}{N}\ln W. \tag{29}$$

The density and current of polymers are given by

$$\rho(\mathbf{r},s) = q^\dagger(\mathbf{r},s)q(\mathbf{r},s) \tag{30}$$

and

$$\mathbf{j}(\mathbf{r},s) = -\frac{D}{2}\Big(q^\dagger(\mathbf{r},s)[\nabla_{\mathbf{r}}q(\mathbf{r},s)] - [\nabla_{\mathbf{r}}q^\dagger(\mathbf{r},s)]q(\mathbf{r},s)\Big), \tag{31}$$

respectively, which satisfy the conservation law

$$\partial_s\rho(\mathbf{r},s) + \nabla_{\mathbf{r}}\cdot\mathbf{j}(\mathbf{r},s) = 0. \tag{32}$$

Here, the $q^\dagger(\mathbf{r},s)$ field satisfies

$$\partial_s q^\dagger(\mathbf{r},s) = -D\nabla_{\mathbf{r}}^2 q^\dagger(\mathbf{r},s). \tag{33}$$

Since the equation of motion for the $q(\mathbf{r},s)$ field differs from that of the $q^\dagger(\mathbf{r},s)$ field, it is convenient to introduce a Nambu-spinor[35]

$$\psi(\mathbf{r},s) = \begin{pmatrix} q(\mathbf{r},s) \\ q^\dagger(\mathbf{r},s)\end{pmatrix}. \tag{34}$$

Then, the generating function can be reformulated as follows

$$W = \int D\psi^\dagger(\mathbf{r},s)D\psi(\mathbf{r},s)\exp\Big\{-\int_0^N ds\int d^3\mathbf{r}\frac{1}{4}\psi^\dagger(\mathbf{r},s)(\partial_s\tau_3 - D\nabla_{\mathbf{r}}^2)\psi(\mathbf{r},s)\Big\}, \tag{35}$$

where the density and current of polymers are expressed by

$$\rho(\mathbf{r},s) = \frac{1}{2}\psi^\dagger(\mathbf{r},s)\psi(\mathbf{r},s) \tag{36}$$

and

$$\mathbf{j}(\mathbf{r},s) = -\frac{D}{4}\Big(\psi^\dagger(\mathbf{r},s)\tau_3[\nabla_{\mathbf{r}}\psi(\mathbf{r},s)] - [\nabla_{\mathbf{r}}\psi^\dagger(\mathbf{r},s)]\tau_3\psi(\mathbf{r},s)\Big) \tag{37}$$

respectively. τ_3 is a Pauil matrix defined as, $\begin{pmatrix} I & 0 \\ 0 & -I\end{pmatrix}$. In this respect the motivation for the

introduction of Nambu-spinor formalism is in dealing with both fields of $q(\mathbf{r},s)$ and $q^{\dagger}(\mathbf{r},s)$ at the same time since density and current are constructed from both fields.

Introducing the chemical potential (μ) and effective interactions (V) of polymers, we can describe interacting polymers at finite density, given by

$$W = \int D\psi^{\dagger}(\mathbf{r},s) D\psi(\mathbf{r},s) \exp\Big[- \int_0^N ds \int d^3\mathbf{r} \Big\{ \frac{1}{4}\psi^{\dagger}(\mathbf{r},s)(\partial_s \tau_3 - \mu - D\nabla^2_{\mathbf{r}})\psi(\mathbf{r},s) + \frac{V}{4}[\psi^{\dagger}(\mathbf{r},s)\psi(\mathbf{r},s)]^2 \Big\} \Big]. \tag{38}$$

Now, we take into account effects of entanglement on polymer dynamics. As performed in the first-quantization representation, we consider the average of two $\delta-$function constraints

$$\begin{aligned} W &= \sum_{N_G=0}^{\infty} \frac{1}{N_G!} \Big\langle \delta\Big(\nabla \times \mathbf{A}(\mathbf{r},s) - \mathbf{j}(\mathbf{r},s) \Big) \delta\Big(N_G - \int d^3\mathbf{r} \mathbf{A}(\mathbf{r},s) \cdot \mathbf{j}(\mathbf{r},s) \Big) \Big\rangle \\ &= \sum_{N_G=0}^{\infty} \frac{1}{N_G!} \int D\psi^{\dagger}(\mathbf{r},s) D\psi(\mathbf{r},s) D\mathbf{A}(\mathbf{r},s) \exp\Big[- \int_0^N ds \int d^3\mathbf{r} \Big\{ \frac{1}{4}\psi^{\dagger}(\mathbf{r},s)(\partial_s \tau_3 - \mu - D\nabla^2_{\mathbf{r}})\psi(\mathbf{r},s) + \frac{V}{4}[\psi^{\dagger}(\mathbf{r},s)\psi(\mathbf{r},s)]^2 \Big\} \Big] \\ &\quad \delta\Big(\nabla \times \mathbf{A}(\mathbf{r},s) - \mathbf{j}(\mathbf{r},s) \Big) \delta\Big(N_G - \int d^3\mathbf{r} \mathbf{A}(\mathbf{r},s) \cdot \mathbf{j}(\mathbf{r},s) \Big), \end{aligned} \tag{39}$$

where N_G is the total number of the Gaussian linking number. Introducing Lagrange multiplier fields in order to exponentiate such $\delta-$function constraints, we rewrite the above expression as follows

$$W = \sum_{N_G=0}^{\infty} \frac{1}{N_G!} \int d\kappa e^{i\kappa N_G} \int DA_\mu(\mathbf{r},s) \int D\psi^\dagger(\mathbf{r},s) D\psi(\mathbf{r},s)$$

$$\exp\Big[-\int_0^N ds \int d^3\mathbf{r}\Big\{\frac{1}{4}\psi^\dagger(\mathbf{r},s)\Big([\partial_s - i\kappa A_s(\mathbf{r},s)\tau_3]\tau_3 - \mu - D[\nabla_\mathbf{r} - i\kappa\mathbf{A}(\mathbf{r},s)\tau_3]^2\Big)\psi(\mathbf{r},s)$$

$$-\kappa^2\frac{D}{4}\psi^\dagger(\mathbf{r},s)\psi(\mathbf{r},s)[\mathbf{A}_\mathbf{r}(\mathbf{r},s)]^2 + \frac{V}{4}[\psi^\dagger(\mathbf{r},s)\psi(\mathbf{r},s)]^2 + i\frac{\theta}{2\pi}\varepsilon_{\mu\nu\lambda}A_\mu(\mathbf{r},s)\partial_\nu A_\lambda(\mathbf{r},s)\Big\}\Big]. \quad (40)$$

Here, κ is the Lagrange multiplier field to impose the Gaussian linking number given by $\delta\Big(N_G - \int d^3\mathbf{r}\mathbf{A}(\mathbf{r},s)\cdot\mathbf{j}(\mathbf{r},s)\Big)$. The "*time*−" ($A_s(\mathbf{r},s)$) and space− ($\mathbf{A}(\mathbf{r},s)$) components of the gauge potential enforce the other $\delta-$function constraint, given by

$$\kappa\rho(\mathbf{r},s) = \frac{\theta}{\pi}\mathbf{B}(\mathbf{r},s),$$

$$\kappa\mathbf{j}(\mathbf{r},s) = \frac{\theta}{\pi}\mathbf{E}(\mathbf{r},s), \quad (41)$$

where $\mathbf{B}(\mathbf{r},s) = \nabla\times\mathbf{A}(\mathbf{r},s)$ and $\mathbf{E}(\mathbf{r},s) = \varepsilon_{\mu\nu\lambda}\partial_\nu A_\lambda(\mathbf{r},s)$ with $\mu = x,\ y,\ z$. In this formulation we allow self-linking of a polymer in addition to mutual entanglement, described by the Chern-Simons term

$$\mathscr{S}_{CS} = \int_0^N ds \int d^3\mathbf{r}\Big(i\frac{\theta}{2\pi}\varepsilon_{\mu\nu\lambda}A_\mu(\mathbf{r},s)\partial_\nu A_\lambda(\mathbf{r},s)\Big), \quad (42)$$

where θ is a statistical angle, which can be used as a phenomenological parameter. By substituting the time derivative ∂_t into the segment derivative ∂_s, we can revisit the previous effective Maxwell-London equation from the effective Chern-Simons field theory.

This field-theoretic formulation allows us to introduce renormalization effects of both dynamics of gauge and polymer fields self-consistently at least at the level of random phase approximation (RPA)[36]. Although this Chern-Simons field theory has a similar structure as that of fractional quantum Hall effect, we can't apply its solution directly. There exists a substantial difference between two Chern-Simons field theories: The time derivative does not have an i factor, where i is a complex number with $i^2 = -1$[37]. Self-consistent renormalizations within the RPA level are required near future.

4 Discussion

Starting from the topological BF theory in the first-quantization representation, we derive an effective Maxwell-London equation. We connect the solution of this phenomenological equation with the physics of the tube model. The essence of the tube model is explained by the Meissner effect of our phenomenological equation. We revisit this formula with an alternative approach based on second quantization. These results seem to be consistent with our numerical analysis.

The entanglement is a dynamical phenomenon originating from the combined effect of polymer connectivity and uncrossability. The dynamics consists of transverse motion, which is confined within a tube, and longitudinal motion, which is represented as reptation. It is important to note that our model assumes the preservation of the linking number and thus quenches the reptation motion to pre-

vent the constraint release. In fact, this approach, that quenches the end points of the test chains, is widely used in simulation to mimic the tube model. Although this assumption (linking number preservation) is enough to describe the formation of tubes, but it is still limited to explain the longitudinal reptation dynamics.

We would like to emphasize that the role of the topological constraint (the preserved Gaussian linking number) differs from that of effective interactions between segments of polymers. Effective interactions between segments of polymers can be translated into dynamics of longitudinal gauge fluctuations, *i.e.*, Coulomb interactions, which would be screened by polymer fluctuations, nothing but the Debye screening in metals[38] and thus, allowed to be neglected at low energies. This massive dynamics of longitudinal gauge fluctuations should be distinguished from Higgs phenomena, where transverse gauge fluctuations become massive, realized in the SC media. The phenomenological Maxwell-London equation implies that the tube model should be understood within the presence of the topological constraint beyond effective interactions between polymer segments.

The Chern-Simons field theory allows us to pursue an analogy between superconductivity and entangled polymer complex in depth. The fundamental concept of U(1) symmetry breaking in superconductivity implies the gapless Goldstone mode and gapped Higgs mode, where the gapless sound mode is pushed up to the plasmon mode when there exist transverse gauge fluctuations[38]. In order to search such plasmon and Higgs modes in the entangled polymer complex, we need to investigate the dynamics of entangled polymers, integrating over gauge fluctuations. This deep connection can be realized in the second-quantization representation. Then, the dynamics of corresponding the plasmon and Higgs modes would reveal characteristic responses of the entangled polymer complex such as compressibility, viscosity, and etc. These will be our future direction.

acknowledgements

The authors thanks to WonBo Lee for helpful discussion in simulation modeling and analysis. KS was supported by the Ministry of Education, Science, and Technology (No. 2012R1A1B3000550 and No. 2011-0030785) of the National Research Foundation of Korea (NRF) and by TJ Park Science Fellowship of the POSCO TJ Park Foundation.YSJ was supported by the Ministry of Education, Science, and Technology (NRF-2012R1A1A2009275, NRF-C1ABA001-2011-0029960) of the National Research Foundation of Korea (NRF).

References

1 E. Witten, *Communications in Mathematical Physics*, 1989, **121**, 351–399.
2 S. C. Zhang, *International Journal of Modern Physics B*, 1992, **6**, 25–58.
3 C. L. Kane and E. J. Mele, *Physical review letters*, 2005, **95**, 146802.
4 S. Edwards, *Proceedings of the Physical Society*, 1967, **91**, 513.
5 F. Tanaka, *Progress of Theoretical Physics*, 1982, **68**, 148–163.
6 F. Ferrari and I. Lazzizzera, *Physics Letters B*, 1998, **444**, 167–173.
7 M. Otto and T. A. Vilgis, *Journal of Physics A: Mathematical and General*, 1996, **29**, 3893.
8 F. Ferrari, *Annalen der Physik*, 2002, **11**, 255–290.
9 R. Everaers, *New Journal of Physics*, 1999, **1**, 12.
10 T. McLeish, *Advances in physics*, 2002, **51**, 1379–1527.
11 S. Edwards, *Proceedings of the Physical Society*, 1967, **92**, 9.
12 M. Doi, S. F. Edwards *et al.*, *The theory of polymer dynamics*, Clarendon Press Oxford, 1986,

vol. 222.
13 P.-G. de Gennes, *The journal of chemical physics*, 1971, **55**, 572–579.
14 L. J. Fetters, A. D. Kiss, D. S. Pearson, G. F. Quack and F. J. Vitus, *Macromolecules*, 1993, **26**, 647–654.
15 H. Watanabe, Y. Matsumiya and T. Inoue, *Macromolecules*, 2002, **35**, 2339–2357.
16 S.-Q. Wang, Y. Wang, S. Cheng, X. Li, X. Zhu and H. Sun, *Macromolecules*, 2013, **46**, 3147–3159.
17 R. M. Robertson and D. E. Smith, *Physical review letters*, 2007, **99**, 126001.
18 B. Wang, J. Guan, S. M. Anthony, S. C. Bae, K. S. Schweizer and S. Granick, *Physical review letters*, 2010, **104**, 118301.
19 J. Glaser, D. Chakraborty, K. Kroy, I. Lauter, M. Degawa, N. Kirchgeßner, B. Hoffmann, R. Merkel and M. Giesen, *Physical review letters*, 2010, **105**, 037801.
20 Q. Zhou and R. G. Larson, *Macromolecules*, 2006, **39**, 6737–6743.
21 N. Y. Kuzuu and M. Doi, *Journal of Polymer Science: Polymer Letters Edition*, 1980, **18**, 775–780.
22 R. Everaers, S. K. Sukumaran, G. S. Grest, C. Svaneborg, A. Sivasubramanian and K. Kremer, *Science*, 2004, **303**, 823–826.
23 D. M. Sussman and K. S. Schweizer, *Physical review letters*, 2011, **107**, 078102.
24 D. M. Sussman and K. S. Schweizer, *Physical review letters*, 2012, **109**, 168306.
25 S. F. Edwards, *Proceedings of the Physical Society*, 1965, **85**, 613.
26 In BF, B means a gauge field and $F = \nabla \times A$ expresses a field strength tensor. An important point is that the gauge field A in F differs from B. On the other hand, the Chern-Simons term can be referred to as AF with $F = \nabla \times A$.
27 G. Y. Cho and J. E. Moore, *Annals of Physics*, 2011, **326**, 1515–1535.
28 Meissner effect is an essential property of superconductivity. Applying magnetic fields, dissipationless supercurrents are induced to screen them perfectly within the London penetration depth, where supercurrents are allowed to flow.
29 M. E. Peskin and D. V. Schroeder, *An introduction to quantum field theory*, Westview, 1995.
30 A. M. Tsvelik, *Quantum field theory in condensed matter physics*, Cambridge university press, 2006.
31 R. Auhl, R. Everaers, G. S. Grest, K. Kremer and S. J. Plimpton, *The Journal of chemical physics*, 2003, **119**, 12718–12728.
32 R. Everaers, S. K. Sukumaran, G. S. Grest, C. Svaneborg, A. Sivasubramanian and K. Kremer, *Science*, 2004, **303**, 823–826.
33 K. Kremer, S. K. Sukumaran, R. Everaers and G. S. Grest, *Computer physics communications*, 2005, **169**, 75–81.
34 M. W. Matsen, *Soft Matter*, 2006, **1**, 87–178.
35 J. Bardeen, L. N. Cooper and J. R. Schrieffer, *Physical Review*, 1957, **108**, 1175.
36 P. W. Anderson, *Physical Review*, 1958, **112**, 1900.
37 Recall that the same factor of i difference in the time-derivative term appears in analogy between the Gaussian chain under the external field and the Schrodinger equation.
38 A. Altland and B. D. Simons, *Condensed matter field theory*, Cambridge University Press, 2010.

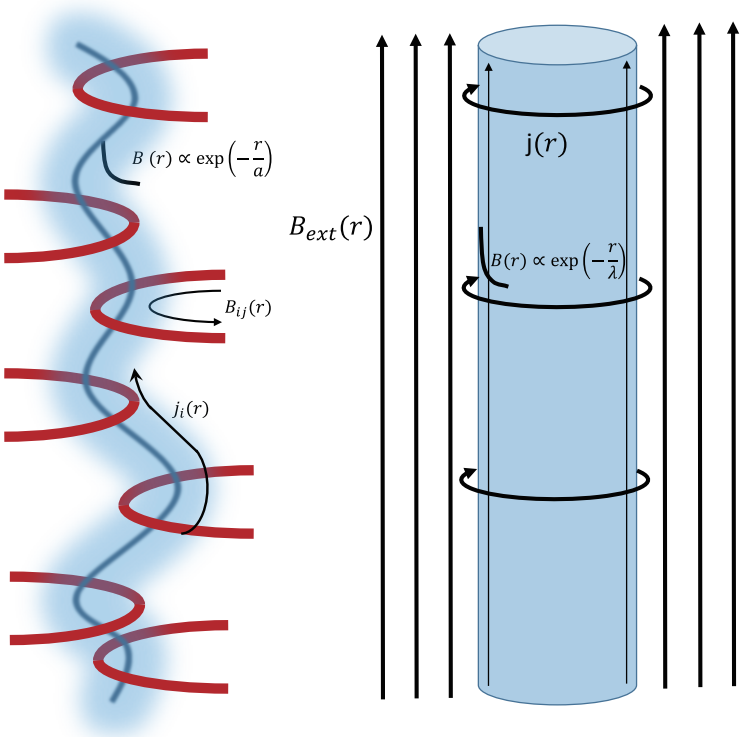

Entangled polymer is analogous to the Higgs phenomena. The preserved linking number of entangled polymer restricts the transverse motion of the test polymer, which corresponds the microscopic picture of the tube model.